Proceedings of the Combustion Institute 40 (2024) 105681

Contents lists available at ScienceDirect

Proceedings of the Combustion Institute

journal homepage: www.elsevier.com/locate/proci

Analysis of spontaneous ignition of hydrogen-enriched methane in a rectangular tube

Shangyong Zhou [a], Jianjun Xiao [b,*], Zhenmin Luo [a,*], Mike Kuznetsov [b], Zheng Chen [c], Thomas Jordan [b], Daniel T. Banuti [b]

[a] School of Safety Science and Engineering, Xi'an University of Science and Technology, Xi'an, Shaanxi 710054, PR China
[b] Institute for Thermal Energy Technology and Safety, Karlsruhe Institute of Technology,76021 Karlsruhe, Germany
[c] College of Engineering, Peking University, Beijing 100871, PR China

ARTICLE INFO

Keywords:
Spontaneous ignition
Hydrogen-enriched methane
Shock wave
Large eddy simulation
GASFLOW-MPI code

ABSTRACT

This study investigates the spontaneous ignition of high-pressure hydrogen-enriched methane in air within a rectangular tube. A computationally efficient approach has been adopted, utilizing a reduced reaction mechanism and ignition delay model within a 3D Large Eddy Simulation (LES) framework. This approach overcomes the limitations of traditional 1D and 2D simulations with detailed chemistry models, which are unable to accurately reproduce the complex 3D shock wave structures within the tube. The simulated shock wave behavior during 9 MPa hydrogen leakage (case 1) and 11 MPa 90 vol% hydrogen/10 vol% methane mixture leakage (case 2) are found to agree well with experimental observations. In case 2, the hot spots generated by reflected shock waves and Mach reflections ignite the hydrogen/methane-air mixture, resulting in three sequential spontaneous ignitions. The flame is observed to primarily propagate along the tube corners and wall centers, with the central ignition spreading across the entire cross-section. For the 25 MPa 24 vol% hydrogen/76 vol% methane mixture leakage (case 6), the shock intensity is significantly reduced due to the increased methane proportion, leading to spontaneous ignition only at the tube corners when the hemispherical shock wave reflects from the wall. The flame predominantly forms downstream along the tube corner, gradually spreading along the tube wall. It is indicated that while the probability of spontaneous ignition decreases with increasing methane content, the risk remains significant under sufficiently high pressures. To the best our knowledge, this study represents the first 3D large eddy simulation of spontaneous ignition for high-pressure hydrogen-enriched methane leakage into air, providing valuable insights into the underlying physical phenomena.

1. Introduction

Hydrogen, as a clean source of energy, has been highly valued for over a century and has been acclaimed as a potential savior for the issues of climate change and the energy crisis [1]. Nevertheless, safe transportation and storage of hydrogen challenge its widespread application. Presently, one of the most cost-effective and well-established methods for transporting and storing hydrogen is via high-pressure storage [2]. Due to the absence of dedicated pipelines for high-pressure hydrogen transport, it is primarily transported on the road which is inefficient and coupled with the potential safety issues [3]. One plausible option for long-distance transport of hydrogen is as natural gas blend through the well-established gas pipeline networks. It has been clearly demonstrated the immense prospects of this technical scheme [4].

High-pressure hydrogen may have a strong propensity for spontaneous ignition upon leakage [5]. Despite the addition of CH_4 having being shown to significantly reduce the spontaneous ignition tendency from H_2, the risk of spontaneous ignition still remains when dealing with high-pressure H_2/CH_4 mixtures [6,7]. Such ignition typically stems from reflected shock waves or intricate vortex rings, necessitating a high-resolution numerical model to accurately reproduce the complex structure of multidimensional shock wave and transient flow fields for exploring the mechanisms.

High-pressure hydrogen spontaneous ignition has been previously investigated using Large Eddy Simulation [8] (LES) and k-epsilon [9] (k-ε) turbulence models, in conjunction with comprehensive chemical reaction mechanisms comprising 18-step [10] and 20-step [11] processes. Detailed chemical kinetics mechanisms have been applied in few

* Corresponding authors.
E-mail addresses: jianjun.xiao@kit.edu (J. Xiao), zmluo@xust.edu.cn (Z. Luo).

https://doi.org/10.1016/j.proci.2024.105681
Received 2 December 2023; Accepted 19 July 2024
Available online 31 July 2024

zero- and one-dimensional combustion calculations [12,13] to study on the spontaneous ignition during high-pressure H_2/CH_4 mixture leakage. The extremely complex H_2/CH_4 detailed chemical reaction mechanism, exemplified by models such as GRI Mech 3.0 [14] (53 species, 325 reactions), USC Mech II [15] (114 species, 784 reactions), and Aramco Mechanism v1.3 [16] (124 species, 766 reactions), poses significant challenges for conducting 3D CFD simulations of H_2/CH_4 spontaneous ignition in air. The practical settings with complex 3D geometry and shock wave structures necessitate simplifications in chemical kinetics. Additionally, solving the multitude of transport equations for various species and addressing the numerical stiffness associated with species source terms in H_2/CH_4 reactions significantly increases computational demands. Therefore, the 3D modeling of spontaneous ignition due to the leakage of high-pressure H_2/CH_4 mixture remains an unexplored area of research.

This study pioneers a practical and efficient approach within the LES framework of the 3D all-speed CFD code GASFLOW-MPI [17] for modeling spontaneous ignition caused by the sudden release of high-pressure H_2, H_2/CH_4 mixtures, or CH_4. Based on the numerical approach, the spontaneous ignition mechanisms during high pressure H_2/CH_4 mixture leakage into air have been analyzed for both hydrogen-dominated and methane-dominated scenarios.

2. Numerical approach

This paper presents an induction time model into the global reaction mechanism to describe the induction phase of spontaneous ignition during high-pressure H_2/CH_4 mixture leakage in a rectangular tube. This approach avoids the computational expense of complex detailed chemical kinetic mechanisms, enabling efficient simulations of spontaneous ignition of non-premixed H_2/CH_4 and air mixtures.

2.1. Governing equations

CFD code GASFLOW-MPI solves 3D compressible Navier- Stokes equations using the robust ICE'd ALE solution algorithm for flows at all speed [17]. For this discussion, a simplified equation set is employed considering the source term due to combustion only.

The mixture mass conservation equation can be written as:

$$\frac{d}{dt}\int_V \overline{\rho} dV = \oint_S -\overline{\rho}\widetilde{\mathbf{u}} dS, \tag{1}$$

where V is the fluid control volume, S is the control surface, and $\mathbf{u}$ is the gas velocity vector.

The transport equation for individual species is given by:

$$\frac{d}{dt}\int_V \overline{\rho_\gamma} dV = \oint_S \left[-\overline{\rho_\gamma}\widetilde{\mathbf{u}} - \mathbf{J}_\gamma\right] dS + \int_V \overline{S}_{\rho,\gamma,com} dV, \tag{2}$$

where γ is the gas species, $\overline{\rho}_\gamma$ denotes the macroscopic density of each specie, $\mathbf{J}_\gamma$ is the diffusion term of species γ, and $S_{\rho,\gamma,com}$ represents the change of species mass due to the combustion.

The momentum conservation equation can be written as:

$$\frac{d}{dt}\int_V \overline{\rho}\widetilde{\mathbf{u}} dV = \oint_S \left[-\overline{\rho}\widetilde{\mathbf{u}}\widetilde{\mathbf{u}} - \overline{P} - \boldsymbol{\tau}\right] dS + \int_V \overline{\rho}\mathbf{g} dV, \tag{3}$$

where P is the pressure, $\boldsymbol{\tau}$ is the viscous stress tensor and $\mathbf{g}$ is the gravitational vector.

The equation of change for total internal energy is:

$$\frac{d}{dt}\int_V \overline{\rho}\widetilde{I} dV = \oint_S \left[-\overline{\rho}\widetilde{I}\widetilde{\mathbf{u}} - \overline{P}\widetilde{\mathbf{u}} - \overline{\mathbf{q}}\right] dS + \int_V \overline{S}_{I,com} dV, \tag{4}$$

where I is the specific internal energy, $\mathbf{q}$ denotes the energy flux vector, and $S_{I,com}$ is the energy source term due to the combustion.

2.2. Turbulence model

The Smagorinsky model is utilized to calculate the subgrid scale turbulent viscosity, which can be expressed as:

$$\mu_t = \overline{\rho} L_S^2 |S|. \tag{5}$$

The mixing length of the subgrid scales, L_s, can be computed as:

$$L_S = C_S \Delta, \tag{6}$$

where C_s is a constant specific to the Smagorinsky model, and Δ represents the LES filter width:

$$\Delta = V^{1/3} = (\Delta x \Delta y \Delta z)^{1/3}. \tag{7}$$

$|S|$ represents an inner product of strain rate tensor, which can be calculated using the following formula:

$$|S| = \sqrt{2\left[\left(\frac{\partial u_x}{\partial x}\right)^2 + \left(\frac{\partial u_y}{\partial y}\right)^2 + \left(\frac{\partial u_z}{\partial z}\right)^2\right] + \left(\frac{\partial u_x}{\partial y} + \frac{\partial u_y}{\partial x}\right)^2 + \left(\frac{\partial u_x}{\partial z} + \frac{\partial u_z}{\partial x}\right)^2 + \left(\frac{\partial u_y}{\partial z} + \frac{\partial u_z}{\partial y}\right)^2}. \tag{8}$$

2.3. Global reaction mechanism

A five-step global reaction mechanism developed by Meredith, et al. [18] has been implemented in GASFLOW-MPI:

$$2CH_4 + O_2 \rightarrow 2CO + 4H_2 \tag{9}$$

$$2H_2 + O_2 \rightarrow 2H_2O \tag{10}$$

$$2CO + O_2 \rightarrow 2CO_2 \tag{11}$$

$$2H_2O \rightarrow 2H_2 + O_2 \tag{12}$$

$$2CO_2 \rightarrow 2CO + O_2 \tag{13}$$

The reaction rates can be written as:

$$\dot{\omega}_{f,1} = C_{f,1} T^{n_1} e^{\frac{-E_{a1}}{RT}} C_{CH_4}^{1.109} C_{CO_2}^{1.572}, \tag{14}$$

$$\dot{\omega}_{f,2} = C_{f,2} T^{n_2} e^{\frac{-E_{a2}}{RT}} C_{H_2}^{1.063} C_{O_2}^{1.363}, \tag{15}$$

$$\dot{\omega}_{f,3} = C_{f,3} T^{n_3} e^{\frac{-E_{a3}}{RT}} C_{co}^{1.318} C_{O_2}^{1.601}, \tag{16}$$

$$\dot{\omega}_{f,4} = C_{f,4} T^{n_4} e^{\frac{-E_{a4}}{RT}} C_{H_2O}^{1.242}, \tag{17}$$

$$\dot{\omega}_{f,5} = C_{f,5} T^{n_5} e^{\frac{-E_{a5}}{RT}} C_{CO_2}^{1.507}. \tag{18}$$

The values of the model constants C_f, n and the activation energy, E_a,

are given in reference [18].

2.4. Induction time model

To overcome the limitations of the global reaction mechanism in capturing the induction phase of spontaneous ignition, an induction time model has been implemented. The transport equation of the induction parameter, α, can be written as:

$$\frac{d}{dt}\int_V \overline{\rho}\widetilde{\alpha}dV = \oint_s \left[-\overline{\rho}\widetilde{u}\widetilde{\alpha} + \left(\frac{\mu}{Sc} + \frac{\mu_t}{Sc_t}\right)\nabla\widetilde{\alpha}\right] dS + \int_V \overline{S}_\alpha dV, \tag{19}$$

where μ is the dynamic viscosity, Sc is the Schmidt number. The value of α varies between 0 and 1. The heat of combustion during the induction phase ($\alpha < 1$) is assumed to be zero, and consequently the source term in the energy conservation equation, $S_{I,com}$, is not affected. When α reaches 1, the induction phase ends and the exothermal reaction starts. The source term in Eq. (21), S_α, is calculated as:

$$\overline{S}_\alpha = \frac{\overline{\rho}}{\tau_{ind}}, \tag{20}$$

where τ_{ind} is the induction time which is a function of mixture composition, pressure P, and temperature T. The induction time model developed by Sichel et al. [19] has been used in this study:

$$\tau_{ind} = A_\alpha \frac{T}{P} exp\left[-B_\alpha + \frac{C_\alpha}{T} + D_\alpha \left(\frac{P}{P_{atm}}\right)^2 exp\left(\frac{T_{a,\alpha}}{T}\right)\right], \tag{21}$$

where A_α, B_α, C_α, D_α and $T_{a,\alpha}$ are the model constant coefficients, as seen in Table 1.

Given the substantially heightened chemical reactivity of hydrogen relative to methane, the ignition process of H_2/CH_4 mixture is primarily initiated by the oxidation reaction of hydrogen, which triggers the initial ignition event. Essentially, it is the reaction of hydrogen that precedes and facilitates the ignition of methane combustion (Figure S1). Furthermore, leveraging the detail chemical kinetic mechanism (GRI-Mech 3.0) within the CHEMKIN-2022 framework, we quantitatively assessed the influence of methane concentration and initial temperature on the ignition delay time. The findings underscored the significance of initial temperature over methane concentration in governing the ignition delay time (Figure S2 and S3). Consequently, the ignition delay time model was confined to solely capturing the oxidation reaction dynamics of hydrogen in this study.

In Sichel et al's study [19], a comparative analysis was conducted between the ignition delay time predictions derived from the induction time model and those obtained using the detail chemical kinetic mechanism, across varying initial pressures (0.1–10 MPa) and temperatures (1000–1600 K). Despite a modest increase in error associated with rising initial pressures, the overall error remained negligible, thereby confirming the reliability of the induction time model. In this study, the ignition conditions were confined to initial pressures below 5 MPa and temperatures within the 1000–1300 K range, which falls well within the applicability spectrum of the model.

Table 1
Induction time model constants.

Model constants	Value
A_α	5.5×10^8 $[Pa\ K^{-1}S]$
B_α	35.1715
C_α	35.1715 $[K]$
D_α	7.22×10^{-11}
$T_{a,\alpha}$	21,205 $[K]$

Fig. 1. Tube for testing spontaneous ignition.

2.5. Simulation setup

Kim's [20] experimental data (9 MPa pure H_2) and our experimental data (11 MPa 90 %H_2/10 %CH_4) were used to validate the models in this study. Both of these experiments were conducted on a 300 mm long rectangular tube with a cross section of 10 mm * 10 mm, as shown in Fig. 1. It is showed that the spontaneous ignition occurred in the first half of the tube (0~150 mm). The high-pressure gases tank was connected to the rectangular tube via a 10 mm diameter cylindrical tube. To save the computational effort, the geometric configuration of the ¼ rectangular tube was used in the calculation, as shown in Fig. 2. The length of the simulated tube was set to 150 mm. The high-pressure tank was simplified as a cylindrical tube. The rupture discs used in the experiments were set up with circular attenuation slots, which burst entirely when the pressure exceeded their burst pressure. Since the transition from a cylindrical to a rectangular tube has a more significant impact on the shock wave than the rupture disc burst process, it was assumed in our study that the rupture disc immediately opened at 0 μs.

The rectangular tube was initially filled with air at a temperature of 300 K and a pressure of 1.0 bar. The end of the tube was set as a pressure boundary. Table 2 provides the initial conditions for the high-pressure zone. The two adjacent walls were set as non-slip and adiabatic walls in the simulation. The tube cross-section was assumed to be symmetrical along the Y and Z axes, and these two symmetrical surfaces were set as free-slip walls, and the symmetry planes are located at $z = 5$ mm and $y = 5$ mm. The analysis of computational domain symmetry effects was conducted and is presented in the Supplementary Figure S4 and Figure S5. We understand that LES is essentially three dimensional. Since the flow in the tube is supersonic, the turbulence effects on the symmetric surfaces become less significant than on the boundary layer of the tube walls.

In the X-direction, the mesh was refined at the rupture disc and gradually stretched towards the end of the tube. It consisted of 2200 meshes, with a minimum mesh size of 50 μm at the rupture disc and a maximum mesh size of 100 μm at the tube's end. In the Y- and Z-directions, the mesh was refined at the tube wall and stretched towards the tube center. It consisted of 80 meshes, with a minimum mesh size of 50 μm at the wall and a maximum mesh size of 75 μm at the tube center. The grid-independence analysis can be found in the Supplementary Figure S6.

3. Results and discussions

In Section 3.1, the measured and calculated pressure and speed of the shock wave due to the sudden release of high-pressure H_2 and H_2/CH_4 mixtures (case 1 and 2) are compared. Then the spontaneous ignition of H_2/CH_4 mixtures (case 2) is investigated in Section 3.2. The methane-dominated H_2/CH_4 mixture at various pressures (case 3–6) are discussed in Section 3.3.

3.1. Numerical model validation

In the experiment of 9 MPa pure H_2 leakage [20], the first pressure sensor was installed at 57 mm away from the rupture disc in the middle of the tube. The second and third pressure sensors were placed at a distance of 28 mm intervals. These three pressure sensors were named as P_1, P_2, and P_3. In our experiment of 90 %H_2/10 %CH_4 leakage at 11 MPa, the first (P_{S1}) and second (P_{S2}) pressure sensors were installed at

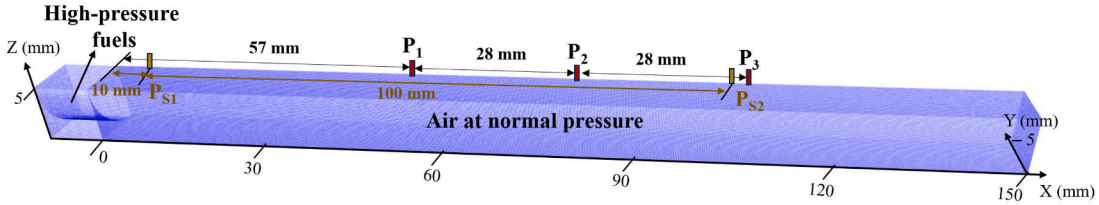

Fig. 2. Geometric configuration of the rectangular tube.

Table 2
The initial conditions in the high-pressure zone.

Cases	H_2	CH_4	Pressure
1	100 vol%	0 vol%	9 MPa
2	90 vol%	10 vol%	11 MPa
3	24 vol%	76 vol%	9 MPa
4	24 vol%	76 vol%	15 MPa
5	24 vol%	76 vol%	20 MPa
6	24 vol%	76 vol%	25 MPa

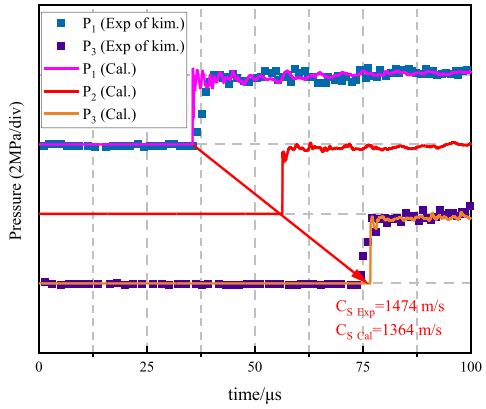

Fig. 3. Comparison of pressure time history at each pressure sensor with experiment data [20] (9 MPa pure H_2).

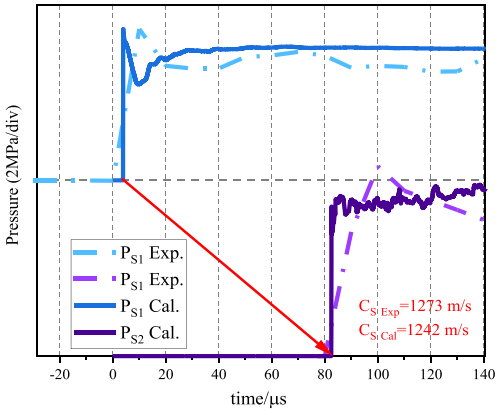

Fig. 4. Comparison of pressure time history at each pressure sensor with experiment data (11 MPa 90 % H_2/10 % CH_4).

10 mm and 110 mm away from the rupture disc. Due to noise interference, the experiment of Kim et al. did not take P_2 into consideration, and the rupture disc open time wasn't defined. Therefore, Fig. 3 is plotted with the moment of pressure rise at P1 as the reference point.

As showed in Fig. 3 and Fig. 4, the calculated pressure of the shock wave at the sensors agree well with the measured ones. By measuring the time difference between the pressure surge instances at P_1 and P_3 or

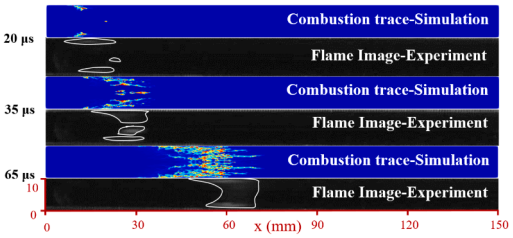

Fig. 5. Comparison of the combustion trace with experimental observation (11 MPa 90 % H_2/10 % CH_4).

P_{S1} and P_{S2}, the velocity of the shock wave can be derived. The measured velocity of 9 MPa pure H_2 is 1474 m/s, while the calculated one is 1364 m/s, resulting in a relative error of roughly 7.5 %. The experimentally obtained velocity of 11 MPa 90 % H_2/10 % CH_4 is 1273 m/s, while the numerical one is 1242 m/s, resulting in a relative error of roughly 2.5 %. The errors can be attributed to the neglect of the detailed rupture process in the numerical calculation.

The water vapor distribution cloud obtained from the CFD simulation and the flame image captured in the experiment at 20 μs, 35 μs and 60 μs are displayed in Fig. 5. This comparison demonstrates that the water vapor distribution closely resembles the flame image, which validates the reasonableness and reliability of the adopted global reaction mechanism combined with the induction time model.

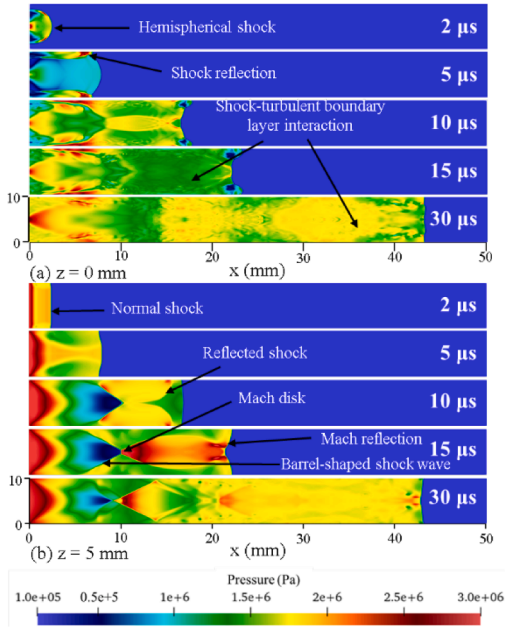

Fig. 6. Shock wave within the tube.

3.2. 11 MPa 90% H_2/10% CH_4 mixture leakage

3.2.1. Characteristics of flow field evolution

Fig. 6 shows the process of generation and development of shock waves, as well as the shock – turbulent boundary layer interaction in the tube. There is a distinct difference in the evolution of pressure between the tube wall ($z = 0$ mm) and the tube center ($z = 5$ mm). As shown in Figure 6(a), after the rupture disc is opened, a hemispherical shock wave was firstly formed above the tube wall ($z = 0$ mm) after 2 μs. When they moved further and reflected on the walls, high-pressure region occurred at the tube corners at 5 μs. Subsequently, the shock wave reflected between the tube walls and complex reflected shock waves were developed at 10 μs. At 15 μs and 30 μs, turbulence was generated in the flow near the wall. The shock wave's shape is more apparent at the tube center ($z = 5$ mm), as shown in Figure 6(b). The shock waves reflect off the wall surface and move towards the tube center, ultimately converging and forming a Mach disk and barrel-shaped shock wave. As the high-pressure fuel flows downstream over time, reflected shock waves caused by the rectangular tube continue to occur.

3.2.2. Spontaneous ignition behavior during 11 MPa 90% H_2/10% CH_4 mixture leakage

The distribution of the H_2/CH_4 mixture combustion product, water vapor (H_2O), serves as an indicator of the combustion processes. It not only traces the pathways of the combustion reaction but also pinpoints the specific locations where these reactions occur. Fig. 7 illustrates the traces of the combustion products and its temperature distribution at various times. The initial spontaneous ignition is observed at the tube corners at 8.5 μs. Due to the influence of the velocity boundary layer, a portion of the air remains near the wall. This results in the flame propagating exclusively along the wall at 15 μs, and it does not extend towards the tube center following the first spontaneous ignition. It is also the reason why the high-speed photography in the experiment captured a large area of flame, rather than a narrow strip of flame perpendicular to the tube [20]. At 19 μs, the second spontaneous ignition occurred at the center of the tube wall, and then the flame spread to downstream and in the direction to the tube corner. The third spontaneous ignition occurred in the tube center at 20.5 μs, and then the flame

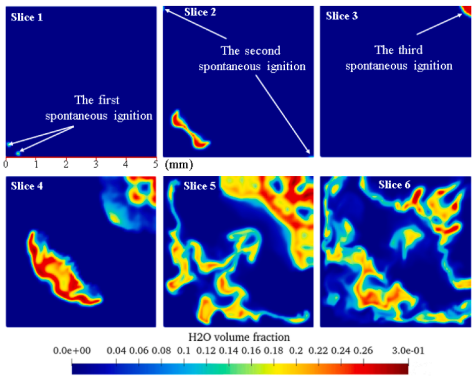

Fig. 8. End view of combustion products distribution (1/4 tube with slice locations shown in Fig. 7).

spread rapidly across the entire cross-section of the tube. The second and third spontaneous ignition is also captured during 9 MPa pure H_2 leakage by the numerical model of Asahara et al.[11]. However, due to their simplification of the structure of high-pressure zone, they didn't capture the first spontaneous ignition that occurred at the tube corners.

Based on the labeled Slice positions shown in Fig. 7, we plotted the cross sections of the H_2O volume fraction at the positions of spontaneous ignition and the combustion front (Fig. 8). As a result, the locations of the three spontaneous ignitions can be shown more accurately. It can also be seen that the first spontaneous ignition at the tube corners cannot spread to the tube center, whereas the third spontaneous ignition at the tube center can spread to the entire contact surface of the fuel jet with the air. In slice 6, the combustion products are not completely distributed throughout the slice due to the folds in the forward flame. Nevertheless, the flames spread over the entire cross section of the tube.

Fig. 9 illustrates the occurrence of three spontaneous ignitions through a visual representation. The cloud map represents the distribution of fuel concentration, while the contour lines depict the pressure field. Notably, the fuel jet exhibits a mixing layer interacting with the surrounding air. When this mixing layer coincides with the high-temperature region caused by the shock wave, spontaneous ignition

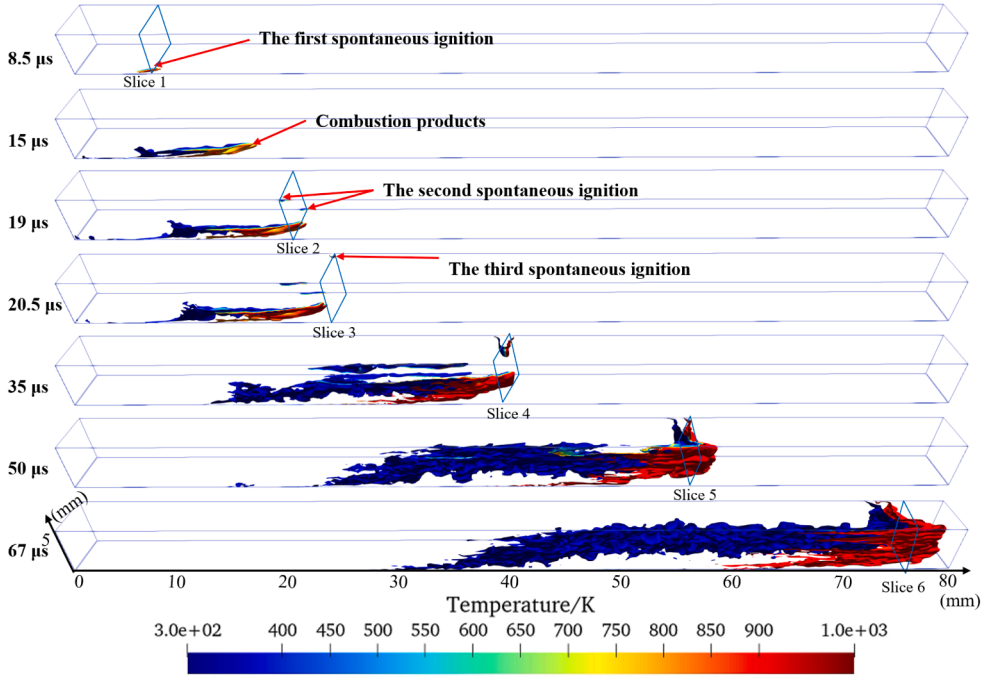

Fig. 7. Combustion products (in blue) and temperature (in color) distribution during 11 MPa 90 % H_2/10 % CH_4 leakage (1/4 tube).

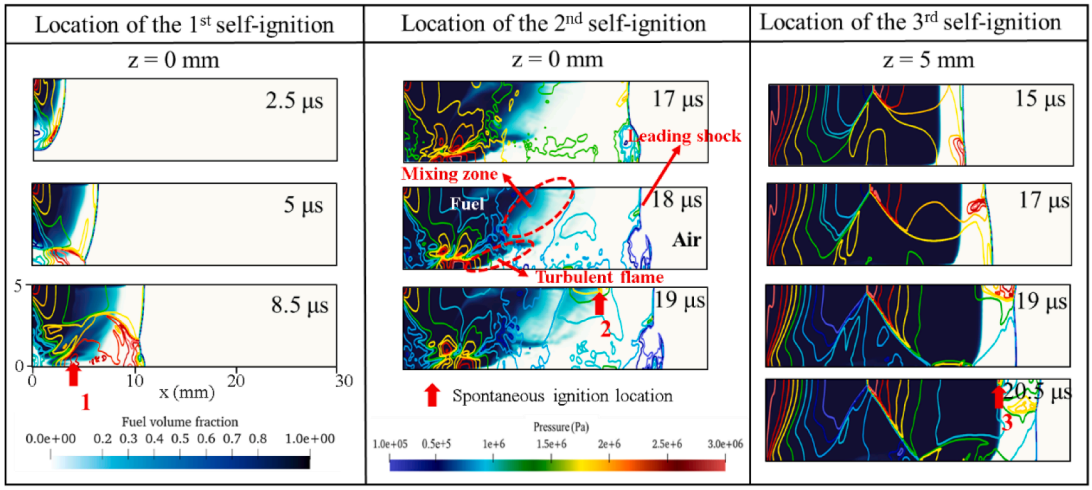

Fig. 9. Shock wave structure and mixing zone development during 11 MPa 90 % H_2/10 % CH_4 mixture leakage.

will be triggered. A hemispherical shock wave was first generated after the rupture disc opens, propagating to the wall and then reflecting back. The reflected shock waves from two neighboring walls met at the tube corners and formed a high-temperature region, which ignited the fuel/air mixture, resulting in the first spontaneous ignition that occurred at the tube corners at 8.5 μs. As the shock wave continued to develop, Mach reflections formed near the tube walls. However, the high-temperature region resulting from Mach reflections failed to ignite at 17 μs since it did not overlap with the fuel/air mixing layer. The combined impact of the fuel jet on the wall and effect of the boundary layer effect led to the formation of a large region of fuel/air mixing layer on the wall, which protruded in the center of the wall. When the reflected shock waves converge at the center of the wall, the high temperature caused by the convergence of the shock waves ignited the fuel/air mixture at 19 μs, resulting in a second spontaneous ignition that occurred at the center of the wall. As shock waves continued to develop, the Mach reflection formed on the tube wall gradually moves towards the tube center. At the same time, the length of the region affected by the Mach reflection grows. As the Mach reflection approached to the tube center, the heated region of the Mach reflection made contact with the fuel/air mixing layer, leading to the third spontaneous ignition at 20.5 μs occurring at the tube center.

3.3. 24% H_2/76% CH_4 mixture leakage

Spontaneous ignition of H_2/CH_4 mixtures, with a composition of 24 % H_2 and 76 % CH_4, at various pressures were studied, as listed in Table 3. Since CH_4 has a lower chemical reactivity and diffusivity than H_2, spontaneous ignition can only be achieved in case 6 when the pressure is adequately high.

3.3.1. Spontaneous ignition behavior during 25 MPa 24% H_2/76% CH_4 mixture leakage

As shown in Fig. 10, spontaneous ignition occurred at the corner of the tube at 8.5 μs. Then the flame propagated downstream along the tube corner, while also spread gradually through the tube wall. Unlike the spontaneous ignition characteristics observed during the 11 MPa 90 % H_2/10 % CH_4 leakage, the 25 MPa H_2/CH_4 mixture leakage into air only resulted in one instance of spontaneous ignition at the tube corners. There was no spontaneous ignition occurred at the wall center and tube center compared to the case of 11 MPa 90 % H_2/10 % CH_4 mixture.

Similar to the Shock wave structure and mixing zone development during 11 MPa 90 % H_2/10 % CH_4 mixture leakage, the reflected shock wave formed by the hemispherical shockwave hit the wall intersected at the tube corners, and formed a high temperature, which led to the ignition of the H_2/CH_4/Air mixture at 8.5 μs. However, the intensity of the Mach reflection, the intersection of the reflected shock wave during 25 MPa 76 % H_2/24 % CH_4 mixture leakage was notably weaker. On the other hand, the 24 % H_2/76 % CH_4 mixture exhibits notably lower chemical reactivity compared to 90 % H_2/10 % CH_4 mixture. As a consequence, the heating generated by the shock wave after 8.5 μs is insufficient to ignite the H_2/CH_4 mixture, resulting in a single spontaneous ignition event occurring at the tube corners.

Since the burst pressure is a key factor in determining the strength of the shock wave, which in turn influences the hot spots inside the rectangular tube that may trigger spontaneous ignition, the phenomena occurring in the rectangular tube vary depending on the burst pressure, as shown in Table 3.

The combustion energy release rate provides insights into the combustion process within the rectangular tube under varying conditions. As illustrated in Fig. 11, no energy release was observed in the tube at the burst pressures of 9 MPa and 15 MPa which is not sufficiently high. However, when the burst pressure was increased to 20 MPa, weak energy release can be obtained at 14 μs and 19 μs, but these were quenched, and a sustained raction did not occur in the tube until 30 μs. Further increasing the burst pressure to 25 MPa successfully triggered the spontaneous ignition reaction at 9 μs. This was followed by a surge in the energy release rate due to the intense combustion of the fuel/air mixing layer at the front of the main jet at 35 μs, which then tended to stabilize after the consumption of the pre-mixed fuel/air mixtures.

The burst pressure has a strong impact on the success of the spontaneous ignition process. Firstly, it amplifies the stirring effect of the shock wave on the fuel-air mixture at the tube walls and corners, promoting enhanced mixing and interaction. Secondly, it elevates the initial temperature of the hot spot for the spontaneous ignition, leading to a substantial increase in the rate of heat release rate during the initial stages of the reaction. It underscores the critical role of burst pressure in controlling the dynamics of spontaneous ignition within the tube.

Table 3
Simulations of ignition at various pressures for leakage of 24 % H_2/76 % CH_4 mixture.

Cases	Pressure	Simulation results
3	9 MPa	No ignition
4	15 MPa	No ignition
5	20 MPa	The first ignition extinguished
6	25 MPa	Ignition successful

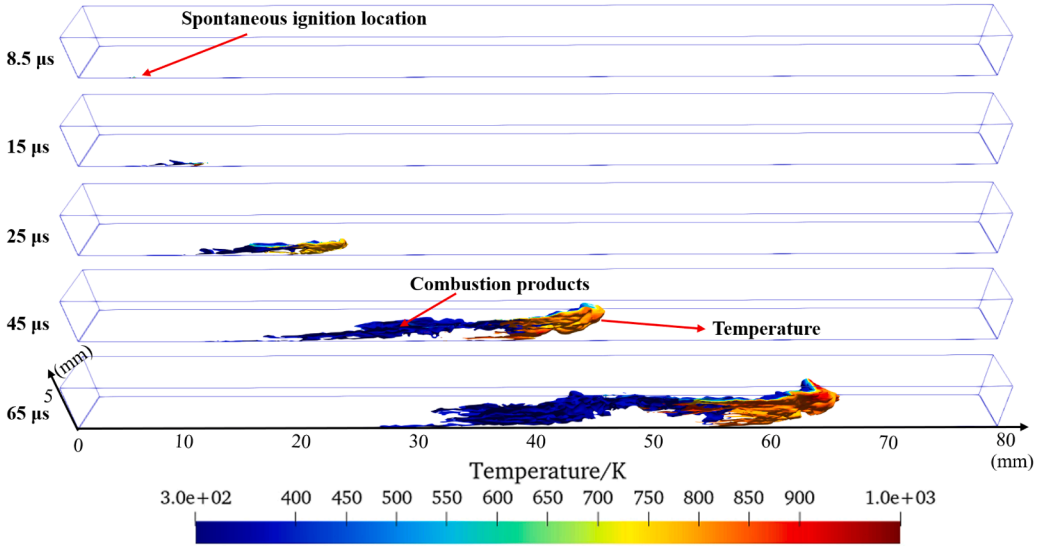

Fig. 10. Combustion products (in blue) and temperature (in color) distribution during 25 MPa 76 % CH_4/24 % H_2 leakage.

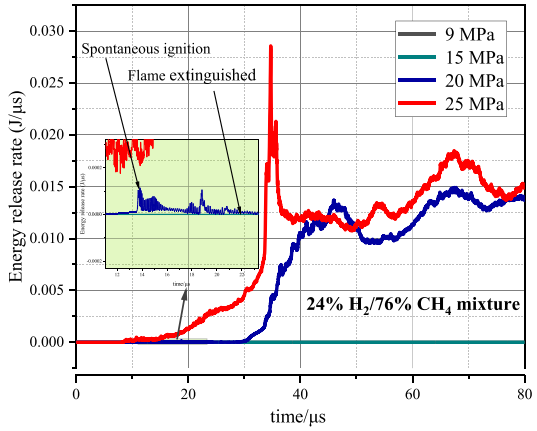

Fig. 11. Heat release rate during 76 % CH_4/24 % H_2 mixture leakage at various burst pressure.

4. Conclusions

To the best knowledge of the authors, this study represents the first evaluation of the spontaneous ignition mechanism of a hydrogen-enriched methane mixture in air using 3D large eddy simulation, providing insights into the underlying physical phenomena. An efficient numerical approach has been developed and validated in the context of large eddy simulation. A practical CFD tool has been adopted to study the gas dynamics and spontaneous ignition phenomena associated with high pressure hydrogen and hydrogen-methane mixture leakages. Utilizing this approach, we have explored spontaneous ignition behavior, achieving detailed capture of shock wave evolution and the characteristics of spontaneous ignition during the leakage in a rectangular tube.

It has been revealed that during the 11 MPa 90 %H_2/10 %CH_4 leakage, the interaction of reflected shock waves at the tube corners and wall center, along with Mach reflections, heated the fuel-air mixture. This sequence led to spontaneous ignitions occurring first at the tube corners, followed by the wall center, and finally at the tube center. Ignitions at the corners and wall center propagated primarily along the tube wall, while the ignition at the tube center expanded along the interface between the main jet and the air, eventually engulfing the entire tube cross-section.

For the 25 MPa 24 % H_2/76 % CH_4 mixture leakage, the shock wave development was analogous to that in 11 MPa 90 % H_2/10 % CH_4 mixture leakage scenarios. However, the shock intensity was reduced due to the methane percentage increases, which inhibited ignition at both the tube wall and center. Spontaneous ignition was confined to the tube corners, with the flame spreading along the tube wall surface and barely reaching the tube center.

Although the likelihood of spontaneous ignition in high-pressure hydrogen-methane mixtures is notably reduced as the methane percentage increases, our study indicates that there is still a potential risk of spontaneous ignition during high-pressure hydrogen-methane leakages. This risk could potentially result in more severe jet fires or explosions, emphasizing the requirements for safety measures to be implemented and considered.

Novelty and Significance Statement

This research pioneers a three-dimensional numerical methodology specifically tailored to model the spontaneous ignition of hydrogen-enriched methane under high-pressure conditions in a rectangular tube. The model overcomes the limitations of traditional 1D and 2D models with detailed chemistry models, which are unable to accurately reproduce the complexities of spontaneous ignition because the accurate 3D predictions of the shock wave structure in the tube is essential. By implementing a validated reduced reaction mechanism together with an ignition delay model, the study successfully reproduce the shock wave dynamics and the subsequent ignition events in a 3D rectangular tube. This development fills the gap in 3D numerical modeling of spontaneous ignition during H_2/CH_4 mixture leakage and provides a robust tool for the analysis such physical phenomena. This study represents the first evaluation of the spontaneous ignition mechanism of a hydrogen-enriched methane mixture in air using 3D large eddy simulation, providing significant insights into the underlying physical phenomena.

CRediT authorship contribution statement

Shangyong Zhou: Writing – original draft, Visualization, Formal analysis. **Jianjun Xiao:** Writing – review & editing, Supervision, Software, Methodology, Investigation, Conceptualization. **Zhenmin Luo:** Writing – review & editing, Project administration. **Mike Kuznetsov:** Writing – review & editing, Formal analysis. **Zheng Chen:** Writing – review & editing, Investigation. **Thomas Jordan:** Writing – review & editing, Project administration. **Daniel T. Banuti:** Writing – review & editing, Project administration.

Declaration of competing interest

The authors declare that they have no known competing financial interests or personal relationships that could have appeared to influence the work reported in this paper.

Supplementary materials

Supplementary material associated with this article can be found, in the online version, at doi:10.1016/j.proci.2024.105681.

References

[1] J.A. Okolie, B.R. Patra, A. Mukherjee, S. Nanda, A.K. Dalai, J.A. Kozinski, Futuristic applications of hydrogen in energy, biorefining, aerospace, pharmaceuticals and metallurgy, Int. J. Hydrogen Energy. 46 (2021) 8885–8905.

[2] J. Zheng, X. Liu, P. Xu, P. Liu, Y. Zhao, J. Yang, Development of high pressure gaseous hydrogen storage technologies, Int. J. Hydrogen Energy. 37 (2012) 1048–1057.

[3] H. Li, X. Cao, Y. Liu, Y. Shao, Z. Nan, L. Teng, et al., Safety of hydrogen storage and transportation: an overview on mechanisms, techniques, and challenges, Energy Rep 8 (2022) 6258–6269.

[4] D. Mahajan, K. Tan, T. Venkatesh, P. Kileti, C.R. Clayton, Hydrogen blending in gas pipeline networks—a review, Energies 15 (2022) 3582.

[5] S. Zhou, Z. Luo, T. Wang, M. He, R. Li, B. Su, Research progress on the self-ignition of high-pressure hydrogen discharge: a review, Int. J. Hydrogen Energ. 47 (2022) 9460–9476.

[6] Q. Zeng, Q. Duan, P. Li, H. Zhu, D. Sun, J. Sun, An experimental study of the effect of 2.5% methane addition on self-ignition and flame propagation during high-pressure hydrogen release through a tube, Int. J. Hydrogen Energ 45 (2020) 3381–3390.

[7] Q. Zeng, Q. Duan, D. Sun, P. Li, M. Zhu, Q. Wang, et al., Experimental study of methane addition effect on shock wave propagation, self-ignition and flame development during high-pressure hydrogen sudden discharge from a tube, Fuel 277 (2020) 118217.

[8] X. Li, L. Teng, W. Li, X. Huang, J. Li, Y. Luo, et al., Numerical simulation of the effect of multiple obstacles inside the tube on the spontaneous ignition of high-pressure hydrogen release, Int. J. Hydrogen Energ. 47 (2022) 33135–33152.

[9] L. Gong, K. Jin, T. Mo, X. Zheng, Y. Yao, Y. Zhang, Numerical investigation on the shock wave propagation, hydrogen/air mixing and spontaneous ignition induced by high-pressure hydrogen release inside the tubes with different shaped cross-sections, Combust. Flame. 252 (2023) 112770.

[10] M.P. Burke, M. Chaos, Y. Ju, F.L. Dryer, S.J. Klippenstein, Comprehensive H_2/O_2 kinetic model for high-pressure combustion, Int. J. Chem. Kinet. 44 (2012) 444–474.

[11] M. Asahara, A. Yokoyama, N. Tsuboi, A.K. Hayashi, Influence of tube cross-section geometry on high-pressure hydrogen-flow-induced self-ignition, Int. J. Hydrogen Energy 48 (2023) 7909–7926.

[12] E. George, P. Magre, V. Sabel'nikov, Numerical simulations of self-Ignition of hydrogen-hydrocarbons mixtures in a hot supersonic air flow, in: 42nd AIAA/ASME/SAE/ASEE Joint Propulsion Conference & Exhibit, Sacramento, California, 2006.

[13] C. Zhong, X. Gou, Inhibition mechanism of CH4 addition on the pressurized hydrogen spontaneous ignition, Energy Fuels 35 (2021) 1715–1726.

[14] G.P Smith, D.M. Golden, M. Frenklach, N.W. Moriarty, B. Eiteneer, M. Goldenberg, et al., GRI Mech 3.0 (2000), http://www.me.berkeley.edu/gri_mech/.

[15] H. Wang, X. You, A.V. Joshi, G.S. Davis, A. Laskin, F. Egolfopoulos, et al., USC mech version II. high-temperature combustion reaction model of H2/CO/C1-C4 compounds (2007), http://ignis.usc.edu/USC_Mech_II.htm.

[16] W.K. Metcalfe, S.M. Burke, S.S. Ahmed, H.J. Curran, et al., A hierarchical and comparative kinetic modeling study of C1 − C2 hydrocarbon and oxygenated fuels, Int. J. Chem. Kinet. 45 (2013) 638–675.

[17] J. Xiao, W. Breitung, M. Kuznetsov, H. Zhang, J.R. Travis, R. Redlinger, GASFLOW-MPI: a new 3-D parallel all-speed CFD code for turbulent dispersion and combustion simulations: part I: models, verification and validation, Int. J. Hydrogen Energ. 42 (2017) 8346–8368.

[18] K. Meredith, D. Black, Automated global mechanism generation for use in CFD simulations, in: 44th AIAA Aerospace Sciences Meeting and Exhibit, Reno, Nevada, 2006.

[19] M. Sichel, N.A. Tonello, E.A. Oran, D.A. Jpnes, A two-step kinetics model for numerical simulation of explosions and detonations in H2-O2 mixtures, Proc. R. Soc. Lond. A 458 (2002) 49–82.

[20] Y.R. Kim, H.J. Lee, S. Kim, I.S. Jeung, A flow visualization study on self-ignition of high pressure hydrogen gas released into a tube, P. Combus. Inst. 34 (2013) 2057–2064.